



Some practical aspects of heat capacity determination by differential scanning calorimetry

Carlos E.S. Bernardes*, Abhinav Joseph¹, Manuel E. Minas da Piedade

Centro de Química Estrutural, Faculdade de Ciências Universidade de Lisboa, Campo Grande, 1749-016, Lisboa, Portugal

ARTICLE INFO

Keywords:

Heat capacity
DSC
Benzoic acid
Sapphire

ABSTRACT

Differential Scanning Calorimetry (DSC) is a widely accessible and versatile method for the determination of the heat capacities of organic materials as a function of temperature. In routine use, it is typically possible to obtain results with an accuracy better than 3 %. However, to achieve this level of accuracy, careful optimization of the experimental procedure for a specific apparatus must be performed. Using benzoic acid as a test substance, this work highlights some practical aspects of heat capacity measurements by DSC, such as crucible material and its geometry, heating rate, thermal lag, the selection of a suitable pre-stabilization stage before the measurement and the duration of the experiment, that can have a strong influence on the quality of the obtained results.

1. Introduction

Heat capacity is a basic thermodynamic property, which is often needed for both fundamental science and technological applications [1,2]. It can, for example, play an important role in the development of pharmaceutical and polymeric materials [3–6], in the validation of molecular simulation methods [7], in the discussion of theories of the crystalline state [8], and in the characterization of biological systems [9]. In general, heat capacity is most accurately determined by adiabatic calorimetry, typically from close to 0 K to ~400 K, when solid organic compounds are studied [1,10–12]. The obtained results can subsequently be used to derive entropy, enthalpy and Gibbs energy functions, as highlighted in several of Professor Gavrichev's works [13–15].

Differential Scanning Calorimetry (DSC) is a widely popularized method to study liquids and solids, which has experienced significant developments in the last 60 years [16–25]. Although not as accurate as adiabatic calorimetry [26,27], it is a versatile and relatively fast method to obtain heat capacities, that requires only a small amount of sample (a few milligrams) [25,26,28]. Techniques for very low (down to ca. 1 K [29]) and high temperatures (e.g. up to 1500 K [29,30]) have been developed, but most measurements are conducted within the range 100 K–700 K [25,26,28].

The determination of heat capacities by DSC is usually carried out in the continuous mode, where a given temperature range is scanned in a single heating step [26,27]. The measurement, involves three

independent experiments, performed sequentially [26,27] (Fig. 1): (i) run 1 (blank run), using empty crucibles with a mass as similar as possible in both the sample and reference cells; (ii) run 2 (calibrant run), with a calibrant material (typically synthetic sapphire), placed in the sample crucible; and (iii) run 3 (sample run), where the calibrant is replaced by a similar weight of the sample under study. In each of these experiments, the same temperature program is employed. It comprises an initial isothermal step (fore period) with duration $t_b - t_a$, at the initial temperature, T_i , followed by a non-isothermal ramp (main period), at a constant rate, to the final temperature, T_f . Finally, a new isothermal step (after period) with duration $t_d - t_c$ is executed at T_f . The lengths of the fore and after periods should be adjusted to ensure that stable heat flow rates are achieved before and after the temperature scan, so that reliable initial and final baselines can be defined [27]. Most often, the extent of the two isothermal steps is set as equal (i.e. $t_b - t_a = t_d - t_c$). To improve the reliability of the results, if possible, the three runs (blank, calibrant, and sample) should be performed with a single pair of sample and reference crucibles and on the same day [27]. While the reference pan can be left untouched, the sample pan is necessarily manipulated between the blank, calibrant, and sample experiments. Its position should, therefore, be kept, as much as possible, constant in all runs, to ensure reproducibility in the pan-calorimeter thermal contacts.

From the obtained curves, Fig. 1, heat capacities, $C_{p,m}(T)$, at a given temperature, T , can be calculated from [26,31]:

$$C_{p,m}(T) = k(T) \cdot \frac{M}{m \cdot \beta} \cdot \Delta\phi(T) \quad (1)$$

* Corresponding author.

E-mail address: cebernardes@fc.ul.pt (C.E.S. Bernardes).

¹ Current address: Division of Research and Development, Lovely Professional University, Phagwara, Punjab, 144411, India.

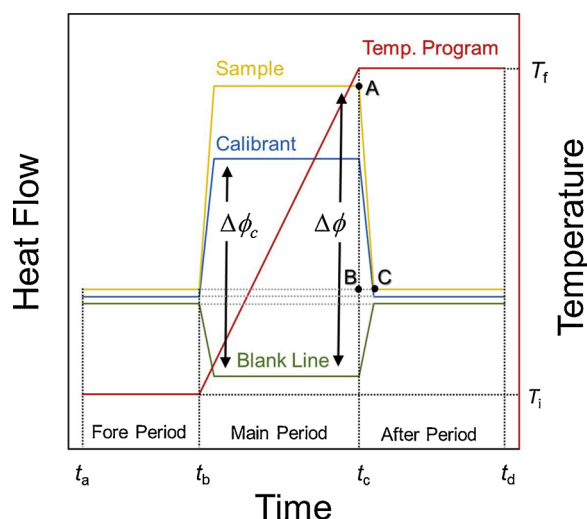


Fig. 1. Schematic representation of the temperature program and heat flow profiles typical of a heat capacity determination by DSC, using the continuous mode of operation.

where m and M are the mass and molar mass of the compound, respectively; β is the heating rate; $\Delta\phi(T)$ is the difference in heat flow rate between the sample and blank runs at a given temperature; and $k(T)$ is a temperature-dependent correction factor, obtained from:

$$k(T) = \frac{C_{p,m}(\alpha\text{-Al}_2\text{O}_3, T)_{\text{Ref}}}{C_{p,m}(\alpha\text{-Al}_2\text{O}_3, T)_{\text{Obs}}} \quad (2)$$

Here, $C_{p,m}(\alpha\text{-Al}_2\text{O}_3, T)_{\text{Ref}}$ represents the recommended heat capacity of sapphire at temperature T and $C_{p,m}(\alpha\text{-Al}_2\text{O}_3, T)_{\text{Obs}}$ is the corresponding experimental value calculated from Eq. (1) with $k = 1$.

Programs for the determination of heat capacities by DSC according to the above-mentioned methodology have been implemented in most software accompanying commercial instruments. They can essentially be used as black boxes, but this normally leads to considerable accuracy loss if the experiments are not carefully designed. Here we discuss some of the pitfalls that can be encountered in the routine determination of heat capacities of organic solids by DSC. Also highlighted are a few details that need to be taken into account to improve the quality of the obtained results. The selected test compound was benzoic acid, which has been recommended as reference material for assessing the accuracy of heat capacity measurements in the temperature range from 10 K to 350 K [32,33]. The following factors were considered in this work: (i) system pre-equilibration, (ii) crucible type, (iii) heating rate, (iv) thermal lag, and (v) temperature interval continuously scanned in a single run.

2. Experimental

Table 1 summarizes the information on the provenance, mass fraction purity, and other relevant characteristics of the materials used in this work.

The heat capacity measurements on benzoic acid in the temperature range 213 K–343 K, were performed with a Netzsch DSC 204 F1 Phoenix apparatus, equipped with a τ -sensor. The apparatus was equipped with a closed-loop intra-cooler system (188 K–873 K) and the whole system was kept at 294 ± 1 K in an air-conditioned room. Nitrogen (Linde N₂ 5.0) was used as a purge and protective gas, at flow rates of $30 \text{ cm}^3 \text{ min}^{-1}$ and $50 \text{ cm}^3 \text{ min}^{-1}$, respectively.

Before use, benzoic acid was reduced to a powder by gentle grinding with pestle mortar. This allowed better packing of the compound inside the pan, thus promoting improved heat transfer between sample, pan and calorimetric system. Note that this operation should not be performed if the material under study can undergo polymorphic transitions

induced by grinding. Sieving, using a mini-sieve micro sieve set (Scienceware, USA), indicated that the ground sample essentially consisted of particles with size $< 250 \mu\text{m}$. A Sapphire disk of 0.25 mm diameter (Netzsch, ref. 6.239.2-91.5.00; $m = 12.69 \text{ mg}$) was used as reference in the heat capacity determination.

The temperature and heat flow scales of the instrument were calibrated at the same heating rates of the heat capacity measurements, using a calibration kit from Netzsch (ref. 6.239.2-91.3.00), consisting of adamantane, indium, tin, bismuth, zinc, and cesium chloride (Table 1). The calibration procedure was previously described [35]. After calibration, the indium fusion temperature onset and enthalpy were $T_{\text{on}} = 429.60 \pm 0.10 \text{ K}$ and $\Delta_{\text{fus}}h_m = 28.90 \pm 0.2 \text{ J g}^{-1}$, respectively (average of 3 measurements; the errors correspond to twice mean absolute deviations). These results agree with the reference values provided by Netzsch for this calibrant: $T_{\text{on}} = 429.75 \text{ K}$ and $\Delta_{\text{fus}}h_m = 28.6 \pm 0.2 \text{ J g}^{-1}$. The instrument control and data treatment were performed with the Netzsch Proteus V. 6.1.0 software. The benzoic acid samples with masses in the range 5 mg–14 mg were contained in either aluminum (40 μL , Perkin Elmer, reference 02190041) or platinum/rhodium (85 μL , Netzsch, references GB399205 and GB399860) crucibles, covered (not sealed) by the companion lids. The mass difference between the empty sample and reference crucibles was smaller than 0.01 mg. All weighings were performed with a precision of $\pm 0.1 \mu\text{g}$ on a Mettler XP2U ultra-micro balance.

The general procedures for heat capacity determination followed the manufacturer recommendations which, in turn, are in accordance with the ASTM E 1269, DIN 51 007, and ISO 11357-4 standards. The temperature program used in the experiments, consisted of an isothermal step at the initial temperature, followed by a temperature ramp at 2 K min^{-1} or 10 K min^{-1} , and a second isothermal step at the final temperature. The duration of the isothermal steps was 20 min for $\beta = 2 \text{ K min}^{-1}$ and 25 min for $\beta = 10 \text{ K min}^{-1}$.

3. Results and discussion

3.1. General

The molar heat capacities, $C_{p,m}$, of benzoic acid were obtained with the Netzsch Proteus V. 6.1.0 software, following the calculation scheme described in the Introduction. They are based on the molar mass M ($\text{C}_7\text{H}_6\text{O}_2$) = $122.123 \text{ g mol}^{-1}$, calculated from the atomic weights recommended by the IUPAC Commission in 2016 [36]. The sapphire ($\alpha\text{-Al}_2\text{O}_3$ disks) heat capacity data used as reference was supplied by Netzsch. Unless otherwise stated, three independent runs using benzoic acid masses between 5 mg and 14 mg, were performed for each investigated experimental condition. No correlation between the sample mass and the obtained values was observed. Therefore, the $C_{p,m}$ values here reported correspond to mean results of three runs and the uncertainties quoted are expanded uncertainties calculated as twice mean absolute deviations.

The relative deviation of the molar heat capacities of benzoic acid obtained in this work, $C_{p,m}$, from the reference data, $C_{p,m}^{\text{ref}}$, was obtained as:

$$s/\% = 100 \cdot \frac{C_{p,m} - C_{p,m}^{\text{ref}}}{C_{p,m}^{\text{ref}}} \quad (3)$$

with

$$C_{p,m}^{\text{ref}}/\text{J K}^{-1} \cdot \text{mol}^{-1} = (0.45785 \pm 0.00082) (T/\text{K}) + (10.369 \pm 0.233) \quad (4)$$

Eq. (4) was derived from a least-squares fit to the benzoic acid heat capacity data reported by Furukawa, Mccoskey and King in the range 215–345 K [37]. The corresponding regression coefficient for 95 % probability was $R^2 = 0.99991$.

The effects of pre-equilibration, crucible type, heating rate, thermal lag, and temperature range scanned in the obtained results are

Table 1

Provenance, temperatures and specific enthalpies of fusion or solid-solid phase transition, and mass fraction purity of the materials used in this work.

Compound	CAS Nr.	Supplier	Reference	T_{fus}/K	$\Delta_{\text{fus}}h/\text{J}\cdot\text{g}^{-1}$	Mass fraction purity
Benzoic acid	65-85-0	Chem-Lab	CL00.0212.0250	395.50 ^a	147.2 ^a	> 0.999 ^b
Sapphire ($\alpha\text{-Al}_2\text{O}_3$ disks)	1344-28-1	Netzsch	6.239.2-91.5.00			0.9999 ^b
Adamantane	281-23-2	Netzsch	1380-K01	208.65 ^{b,c}	22.0 ^{b,c}	≥ 0.99 ^b
Indium ^d	7440-74-6	Netzsch	MKBJ7540V	429.75 ^b	28.6 ± 0.2 ^b	0.99999 ^b
Tin ^d	7440-31-5	Netzsch	121213	505.05 ^b	60.5 ^b	0.99999 ^b
Bismuth	7440-69-9	Netzsch	230112	544.55 ^b	53.1 ^b	0.99999 ^b
Zinc ^d	7440-66-6	Netzsch	05928JN	692.65 ^b	107.5 ^b	0.99999 ^b
Cesium chloride	7647-17-8	Netzsch	160709	749.15 ^b	17.2 ^b	0.99999 ^b
Nitrogen	7727-37-9	Linde	5.0			≥ 0.99999 ^b

^a Ref. [34].^b Given by the supplier.^c Solid-solid phase transition.^d According to German standard DIN 51,007.

addressed in the following sections.

3.2. Pre-equilibration

As mentioned above, each heat capacity measurement involves three runs: blank, calibrant (sapphire in the present work) and sample. It is widely recommended that these experiments are carried out in sequence, on the same day, using the same temperature program, and the same set of crucibles [27]. Less often mentioned is, however, the need to ensure a very stable heat flow rate difference between the sample and reference cells before starting the baseline acquisition. Attention to this detail should be paid, even if the initial temperature of the experiment has been reached and seems to be constant.

Fig. 2 compares the heat capacity results obtained for benzoic acid in the range 220 K–271 K, at a heating rate $\beta = 2 \text{ K}\cdot\text{min}^{-1}$, in a series of

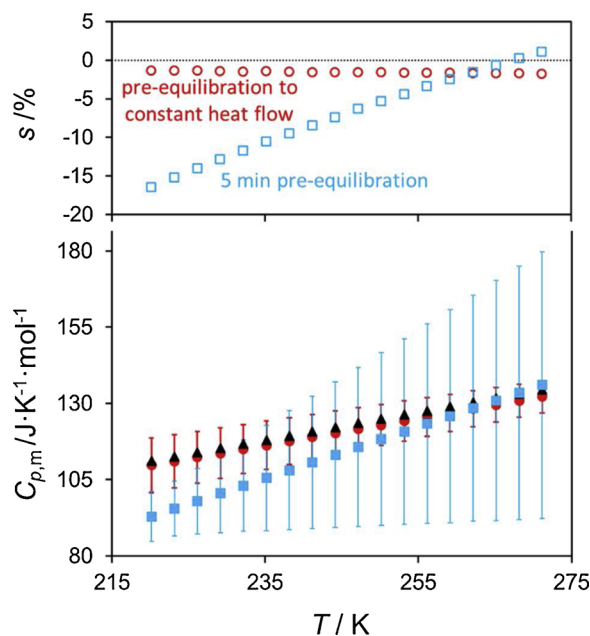


Fig. 2. Comparison of the molar heat capacity, $C_{p,m}$, of benzoic acid in the range 220 K to 271 K, obtained in this work using two different pre-equilibration periods, with reference data given by Eq. (4): (i) closed blue squares: 5 min pre-equilibration; (ii) closed red dots: pre-equilibration until a stable heat flow was observed; (iii) closed black triangles: reference values. The error bars correspond to twice the mean absolute deviation of three independent runs. The open symbols give the deviation (s) of the obtained values relative to the reference data, calculated from Eq. (3). (For interpretation of the references to colour in this figure legend, the reader is referred to the web version of this article.)

experiments where short (c.a. 5 min after reaching T_i) and adequate (until a stable heat flow rate is observed) delays were selected before starting the baseline acquisition. Also shown are the reference values from Furukawa et al. [37] computed from Eq. (4). It can be concluded from Fig. 2 that an insufficient pre-equilibration time leads to: (i) a considerable loss of precision expressed by error bars of up to $\sim 43 \text{ J}\cdot\text{K}^{-1}\cdot\text{mol}^{-1}$, representing $\sim 32\%$ of the measured value; (ii) deviations from the reference data as large as $\sim 16\%$. In contrast, if a constant heat flow rate is ensured before starting the baseline acquisition, very large improvements in precision (the error bars decrease to $9 \text{ J}\cdot\text{K}^{-1}\cdot\text{mol}^{-1}$) and accuracy (the discrepancy to the reference results is reduced to $< 3\%$) are observed. Particularly important to achieve an initial constant heat flow in sub-ambient temperature measurements, is to ensure that the cooler is working at optimal conditions. In the case of the Netzsch DSC 204 F1 Phoenix apparatus used in this work it was found that $T_i = 213 \text{ K}$ could be reached and was apparently stable $\sim 20 \text{ min}$ after turning on the system. The proper stabilization of the intercooler to achieve a steady heat flow signal required, however, at least 60 min.

3.3. Crucible type

The selection of a convenient crucible for the experiments is also an important factor in heat capacity measurements by DSC. For $T < 870 \text{ K}$ (a range suitable for most organic compounds), aluminum crucibles are usually employed. Other materials may, however, be needed if, for example, the sample reacts with aluminum or if higher temperatures need to be reached. A possible alternative is to use crucibles made of Pt/Rh alloy. These have a much better chemical inertness and allow experiments up to 2000 K. However, they suffer from the disadvantage of a thermal conductivity almost eight times smaller than aluminum [38].

To gain some insight into the influence of the crucible type in heat capacity measurements, aluminum and Pt/Rh crucibles of different models (Fig. 3) were used to study benzoic acid in the ranges 213 K–273 K and 298 K–343 K. The heating rate was $\beta = 2 \text{ K}\cdot\text{min}^{-1}$. The obtained results are shown in Fig. 4. This illustration clearly indicates that the best overall performance is achieved with aluminum crucibles, for which deviations $s < 3\%$ relative to the reference data given by Eq. (4) were observed. Measurements with the Pt/Rh pans led to considerably larger deviations (5 % to 13 %). The poorer performance of the Pt/Rh crucibles may, at least in part, be attributed to the lower thermal conductivity mentioned above. But perhaps the most essential factor is the less efficient crucible-sample contact. As shown in Fig. 3, in the case of the aluminum crucible the pan and lid are both in contact with the sample. This is not true, however, for the Pt/Rh crucibles. It is therefore expected that the sample-crucible thermal equilibration and the development of temperature gradients throughout the sample along the heating ramp, will be most notable in the case of Pt/Rh crucibles. The primary importance of this aspect is further supported

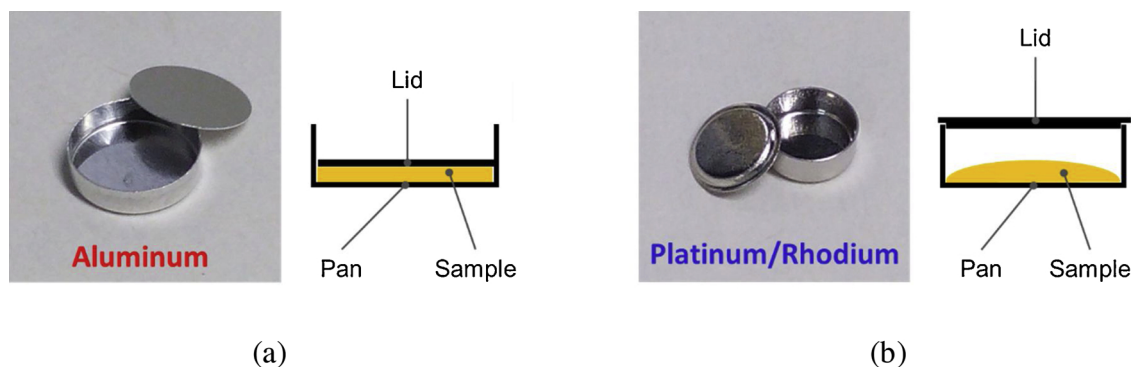


Fig. 3. The (a) aluminum and (b) platinum/rhodium crucibles used in this work, with schemes of the assembled systems with the sample inside.

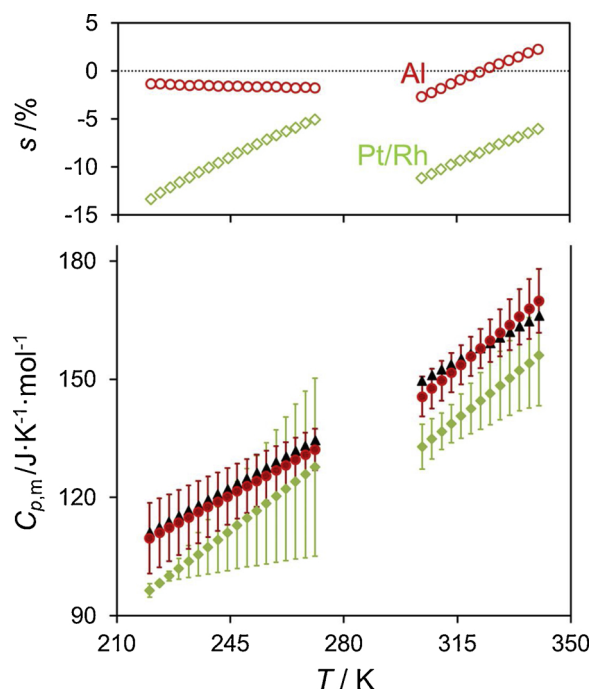


Fig. 4. Comparison of the molar heat capacities, $C_{p,m}$, of benzoic acid in the ranges 213 K to 273 K and 298 K to 343 K, obtained in this work using aluminum (closed red dots) and platinum/rhodium (closed green diamonds) crucibles (see Fig. 3) with the reference data given by Eq. (4) (closed black triangles). The error bars correspond to twice the mean absolute deviation of three independent runs. The open symbols give the mean deviations (s) of the obtained values relative to the reference data, calculated according to Eq. (3). (For interpretation of the references to colour in this figure legend, the reader is referred to the web version of this article.)

by the observation of 5% deviations in heat capacity measurements on benzoic acid carried out on a Perkin Elmer DSC 7, using 20 μL hermetically sealed aluminum pans for volatile compounds (Perkin Elmer, reference 02190062), where a large empty volume exists over the sample [39].

3.4. Heating rate

The heating rate is another key factor to consider in the determination of heat capacity by DSC. Fast heating rates can lead to fast experiments. But it must be ensured that an efficient heat transfer from the calorimeter to the sample is maintained in order to minimize thermal lag effects and temperature gradients within the sample.

Fig. 5a shows a comparison of the heat capacities of benzoic acid obtained at 2 K·min^{−1} and 10 K·min^{−1}, in the temperature ranges 213 K–273 K and 298 K–343 K, using the aluminum crucibles in Fig. 3a.

The results suggest that a smaller overall deviation from the reference values given by Eq. (4) is achieved if the slower heating rate is selected, particularly in the sub-ambient temperature range. The gain is, however, not very significant, since both heating rates lead to $s < 3.1\%$, which is well within the typical uncertainties found for this type of experiment [26,27]. It should, nevertheless, be mentioned that fast heating rates must be used with caution. When the heating ramp starts the instrument changes from an isothermal to a non-isothermal regime and comes back to the isothermal condition when the ramp stops. At these transition periods an initial temperature undershoot and a final temperature overshoot are observed, both of which are considerably larger for 10 K·min^{−1} than for 2 K·min^{−1}. In addition, at least with the equipment used in this work, the final overshoot is always more notable than the initial undershoot. A comparison of the final overshoots observed in experiments carried out at 10 K·min^{−1} and 2 K·min^{−1} is shown in Fig. 5b.

The presence of these undershoot/overshoot effects has three implications: (i) Firstly a longer final isothermal period may be needed at 10 K·min^{−1} than at 2 K·min^{−1}, to ensure a sufficiently large final baseline, corresponding to a constant and linear heat flow trace (Fig. 6b and section 3.5). It follows that (ii) running an experiment at a higher heating rate does not necessarily translate into a significant time-saving. Finally (iii) a higher heating rate may also require a wider temperature ramp, so that a sufficiently long portion of the main period where the heat flow trace is proportional to the heat capacity of the sample is observed. At 10 K·min^{−1}, a 30 K range is covered in only 3 min. It must be ensured that within this time frame the observed heat flow rate is not contaminated by transient effects resulting from temperature undershoots or overshoots and is effectively proportional to the heat capacity of the sample. If not, the computed data may not be meaningful or will exhibit very large errors. The use of smaller heating rates makes the measurements less susceptible to these transient effects.

In conclusion, at least with the instrument used in this work, reliable heat capacity measurements ($s < 3.1\%$) may be obtained at 10 K·min^{−1}, without significant loss in accuracy compared to 2 K·min^{−1}, provided that a suitable methodology is followed.

3.5. Thermal lag

The magnitude of the thermal lag, δT , for different heating rates, β , was estimated from the return of the DSC signal to the baseline after the scanning process, using [40]:

$$\delta T = \frac{\delta A}{m \cdot c_p} \quad (5)$$

Here δA is the “enthalpy lag” calculated from the area defined by the points A, B, and C in Fig. 1, m is the mass and c_p is the specific heat capacity of the sample at T_c (this is normally a good approximation since c_p does not considerably change with temperature in the range from $T_c - \delta T$ to T_c [40]). The obtained results for benzoic acid and the

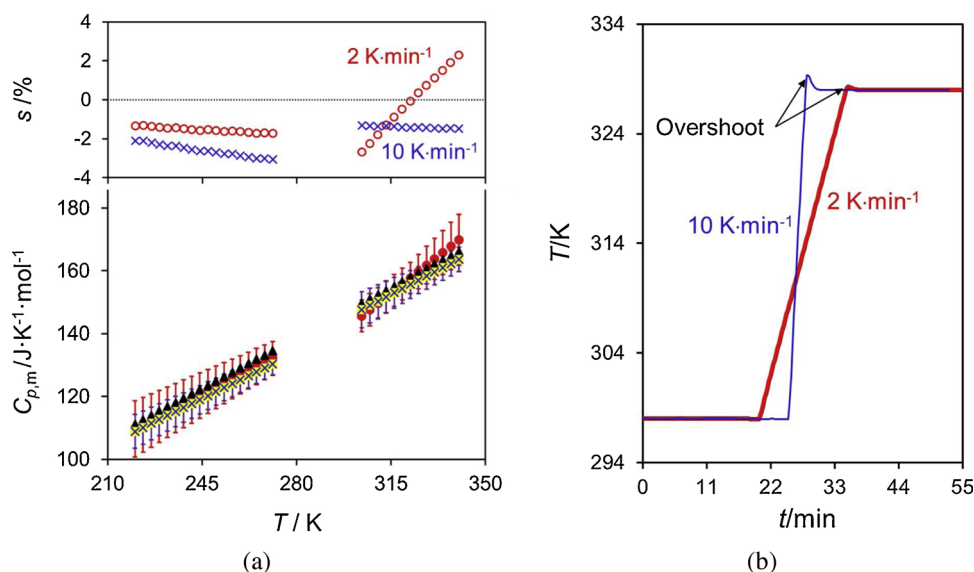


Fig. 5. (a) Comparison of the molar heat capacities, $C_{p,m}$, of benzoic acid in the ranges 213 K to 273 K and 298 K to 343 K, obtained in this work, using aluminum crucibles (see Fig. 3a) at $2\text{ K}\cdot\text{min}^{-1}$ (closed red dots) and $10\text{ K}\cdot\text{min}^{-1}$ (blue crosses in yellow background), with the reference data given by Eq. (4) (closed black triangles). The error bars correspond to twice the mean absolute deviation of three independent runs. The open symbols give the mean deviations (s) of the obtained values relative to the reference data, calculated from Eq. (3). (b) Variation of the sample temperature during the experiments at $2\text{ K}\cdot\text{min}^{-1}$ (red line) and $10\text{ K}\cdot\text{min}^{-1}$ (blue line). (For interpretation of the references to colour in this figure legend, the reader is referred to the web version of this article.)

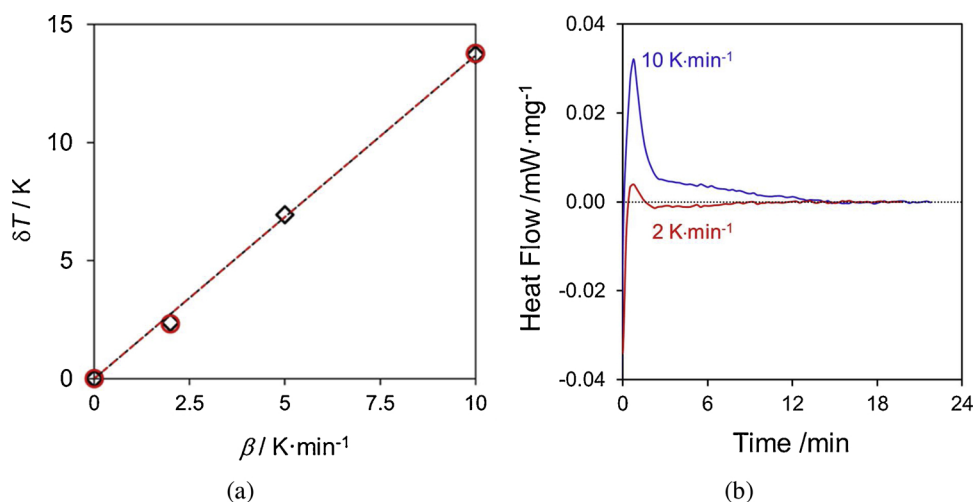


Fig. 6. (a) Thermal lag, δT , at 323 K for the sapphire disk (\diamond) and benzoic acid (\circ) samples ($m \approx 13\text{ mg}$) used in this work, as a function of the heating rate, β . The dotted lines represent the least-squares fitting of the data with interception at the origin. (b) Heat flow profiles obtained after heating a sapphire sample at 2 and $10\text{ K}\cdot\text{min}^{-1}$. The origin of the time scale corresponds to the end of the heating period.

sapphire disk samples with comparable masses are illustrated in Fig. 6a. This figure shows that the thermal lag linearly increases with β and is very similar for both compounds. This suggests that, no significant thermal conductivity differences between the calibrant and sample runs are likely to occur. Moreover, because the thermal lag increases with the heating rate (e.g. $\delta T \approx 2\text{ K}$ for $\beta = 2\text{ K}\cdot\text{min}^{-1}$ and $\delta T \approx 14\text{ K}$ for $\beta = 10\text{ K}\cdot\text{min}^{-1}$) the temperature range covered in the experiments should also proportionally increase with β .

From Fig. 6a it was also possible to obtain $\delta(\delta T)/\delta\beta \approx 1.4\text{ min}$. If an exponential heat transfer behavior is assumed, then the DSC heat flow signal should return to the baseline after approximately $5 \times \delta(\delta T)/\delta\beta = 7\text{ min}$. This was in fact observed in most experiments carried out with the instrument used in this work. In a few cases, however, without an apparent reason, larger equilibration times were needed, particularly at the higher heating rate. This is illustrated in Fig. 6b for a particular case corresponding to $\beta = 10\text{ K}\cdot\text{min}^{-1}$, where an equilibration time of $\sim 15\text{ min}$ was found to be necessary to reach the baseline. For this reason, to ensure that (i) the baseline could be reached and (ii) collected for a sufficiently long period of time, the duration of the fore and after periods were set to 20 min, when $\beta = 2\text{ K}\cdot\text{min}^{-1}$, and 25 min, when $\beta = 10\text{ K}\cdot\text{min}^{-1}$. This stresses the importance of a careful evaluation of the DSC apparatus thermal behavior before starting the heat capacity measurements.

3.6. Temperature range scanned

In the sections above, it became apparent that the acquisition of suitable initial and final baselines could lead to the necessity of longer experiments at $10\text{ K}\cdot\text{min}^{-1}$ than at $2\text{ K}\cdot\text{min}^{-1}$. It follows that the use of fast heating rates only becomes significantly advantageous, in terms of saving time, if large enough temperature ranges are covered.

To evaluate the reliability of scanning a large temperature interval in a single run, covering sub-ambient and above ambient conditions, the heat capacity of benzoic acid was also determined at $10\text{ K}\cdot\text{min}^{-1}$, from 219 K to 341 K (122 K segment), using the aluminum crucibles in Fig. 3a. The obtained results are compared in Fig. 7 with the reference values computed from Eq. (4). It can be concluded from Fig. 7 that by using an optimized procedure a deviation smaller than 3% can still be achieved for a long main period.

4. Final remarks

Although all tests reported in this work refer to benzoic acid and were performed with a Netzsch DSC 204 F1 Phoenix apparatus, the following main conclusions are expected to be transferable for other organic solids and instruments:

- (i) The quality of the heat capacity results obtained by DSC strongly

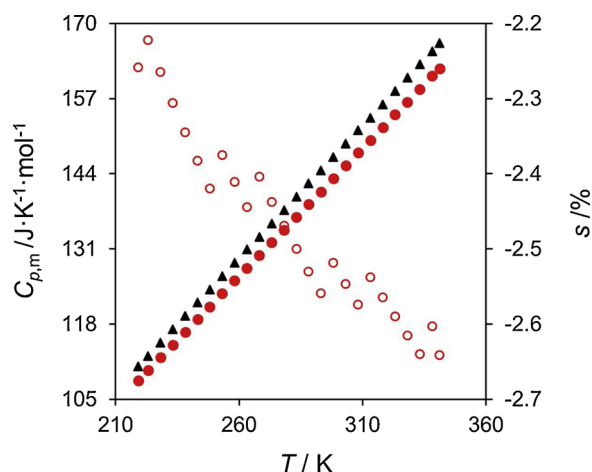


Fig. 7. Comparison of the molar heat capacities, $C_{p,m}$, of benzoic acid obtained in a single run, carried out in the temperature range 219 K to 341 K, at $10\text{ K}\cdot\text{min}^{-1}$ (closed red dots), with the reference data given by Eq. (4) (closed black triangles). The open symbols give the mean deviations (s) of the obtained values relative to the reference data, calculated from Eq. (3). (For interpretation of the references to colour in this figure legend, the reader is referred to the web version of this article.)

depends on the selection of a sufficiently long pre-stabilization stage that ensures a suitable baseline where the heat flow signal is as constant as possible. Observing a constant initial temperature is not a reliable criterion to start the baseline acquisition.

- (ii) The use of crucibles made of materials with high thermal conductivity (e.g. aluminum, gold, or copper) should be preferred, if they do not react with the sample and the temperature range to be covered in the experiments is compatible with the use of these materials.
- (iii) The crucible shape may also be critical to ensure an efficient heat transfer between the sample and the calorimetric cell. Better results are obtained if the sample has an efficient contact with both the crucible pan and lid (top and bottom), so that thermal lag problems and temperature gradients within the sample are minimized. In the case of volatile solids, the use of crucibles where the lid is not in intimate contact with the sample and a significant headspace exists, may also lead to accuracy loss, as the thermal contribution from sublimation will be superimposed with the heat capacity measurement.
- (iv) The selection of the heating rate should be compatible with the range of temperatures covered in the experiment, i.e. higher heating rates may not necessarily correspond to a considerable time saving if the temperature interval scanned is small and reliable results are aimed.
- (v) Last but not the least, before initiating measurements with a specific compound, the temperature program and experimental protocol should always be optimized for the available instrument, using a reference compound such as benzoic acid.

CRediT authorship contribution statement

Carlos E.S. Bernardes: Methodology, Writing - review & editing.
Abhinav Joseph: Investigation. **Manuel E. Minas da Piedade:** Writing - review & editing.

Declaration of Competing Interest

The authors declare that they have no known competing financial interests or personal relationships that could have appeared to influence the work reported in this paper.

Acknowledgments

This work was supported by Fundação para a Ciência e a Tecnologia (FCT), Portugal through Projects PTDC/QUI-OUT/28401/2017 (LISBOA-01-0145-FEDER-028401), UIDB/00100/2020, and UIDP/00100/2020, and a doctoral grant awarded to A. Joseph (SFRH/BD/90386/2012). Thanks are also due to PARALAB (Portugal) for providing the Netzsch DSC 204 F1-Phoenix apparatus.

Appendix A. Supplementary data

Supplementary material related to this article can be found, in the online version, at doi:<https://doi.org/10.1016/j.tca.2020.178574>.

References

- [1] D.R. Stull, E.F. Westrum, G.C. Sinke, *The Chemical Thermodynamics of Organic Compounds*, Wiley, New York, 1969.
- [2] E. Wilhelm, T.M. Letcher, *Heat Capacities: Liquids, Solutions and Vapours*, Royal Society of Chemistry, Cambridge, 2010.
- [3] S.D. Clas, C.R. Dalton, B.C. Hancock, Differential scanning calorimetry: applications in drug development, *Pharm. Sci. Tech. Today* 2 (1999) 311–320, [https://doi.org/10.1016/S1461-5347\(99\)00181-9](https://doi.org/10.1016/S1461-5347(99)00181-9).
- [4] M.M. Knopp, K. Löbmann, D.P. Elder, T. Rades, R. Holm, Recent advances and potential applications of modulated differential scanning calorimetry (mDSC) in drug development, *Eur. J. Pharm. Sci.* 87 (2016) 164–173, <https://doi.org/10.1016/j.ejps.2015.12.024>.
- [5] S.I. Stoliarov, R.N. Walters, Determination of the heats of gasification of polymers using differential scanning calorimetry, *Polym. Degrad. Stabil.* 93 (2008) 422–427, <https://doi.org/10.1016/j.polymdegradstab.2007.11.022>.
- [6] J. McHugh, P. Fideu, A. Herrmann, W. Stark, Determination and review of specific heat capacity measurements during isothermal cure of an epoxy using TM-DSC and standard DSC techniques, *Polym. Test.* 29 (2010) 759–765, <https://doi.org/10.1016/j.polymertesting.2010.04.004>.
- [7] G. Qiao, M. Lasfargues, A. Alexiadis, Y.L. Ding, Simulation and experimental study of the specific heat capacity of molten salt based nanofluids, *Appl. Therm. Eng.* 111 (2017) 1517–1522, <https://doi.org/10.1016/j.applthermaleng.2016.07.159>.
- [8] E.S.R. Gopal, *Specific Heats at Low Temperature*, Heywood Books, London, 1966.
- [9] J. Tang, S. Sokhansanj, S. Yannacopoulos, S.O. Kasap, Specific-heat capacity of lentil seeds by differential scanning calorimetry, *Trans. ASABE* 34 (1991) 517–522, <https://doi.org/10.13031/2013.31693>.
- [10] E.F.J. Westrum, J.P. McCullough, Thermodynamics of crystals, in: D. Fox, M.M. Labes, A. Weissberger (Eds.), *Physics and Chemistry of the Organic Solid State*, John Wiley, New York, 1963, pp. 1–178.
- [11] F. Grønvold, Adiabatic calorimetry and solid-state properties above ambient-temperature, *Pure Appl. Chem.* 65 (1993) 927–934, <https://doi.org/10.1351/pac199365050927>.
- [12] H. Suga, Perspectives of low temperature calorimetry, *Thermochim. Acta* 355 (2000) 69–82, [https://doi.org/10.1016/S0040-6031\(00\)00438-X](https://doi.org/10.1016/S0040-6031(00)00438-X).
- [13] A.V. Tyurin, R.N. Nenashev, K.S. Gavrichiev, V.P. Zlomanov, Thermodynamic functions of vanadyl acetylacetonate $\text{VO}(\text{C}_5\text{H}_7\text{O}_2)_2$ at 0–350 K, *Russ. J. Phys. Chem. A* 89 (2015) 1711–1714, <https://doi.org/10.1134/S0036024415100325>.
- [14] A.V. Tyurin, N.A. Gribchenkova, V.N. Guskov, K.S. Gavrichiev, Thermodynamic properties of aluminum oxynitride from 0 to 340 K, *Inorg. Mater.* 51 (2015) 340–344, <https://doi.org/10.1134/S0020168515040184>.
- [15] K.S. Gavrichiev, N.N. Smirnova, V.M. Gurevich, V.R. Danilov, A.V. Tyurin, M.A. Ryumin, L.N. Komissarova, Heat capacity and thermodynamic functions of LuPO_4 in the range 0–320 K, *Thermochim. Acta* 448 (2006) 63–65, <https://doi.org/10.1016/j.tca.2006.05.019>.
- [16] E.S. Watson, M.J. O'Neill, J. Justin, N. Brenner, A differential scanning calorimeter for quantitative differential thermal analysis, *Anal. Chem.* 36 (1964) 1233–1238, <https://doi.org/10.1021/ac60213a019>.
- [17] M.J. O'Neill, The analysis of a temperature-controlled scanning calorimeter, *Anal. Chem.* 36 (1964) 1238–1245, <https://doi.org/10.1021/ac60213a020>.
- [18] M.J. O'Neill, Measurement of specific heat functions by differential scanning calorimetry, *Anal. Chem.* 38 (1966) 1331–1336, <https://doi.org/10.1021/ac60242a011>.
- [19] I. Hatta, S. Muramatsu, High precision heat capacity measurement by dynamic differential scanning calorimetry, *Jpn. J. Appl. Phys.* 35 (1996) L858–L860, <https://doi.org/10.1143/Jjap.35.L858>.
- [20] J.H. Flynn, Thermodynamic properties from differential scanning calorimetry by calorimetric methods, *Thermochim. Acta* 8 (1974) 69–81, [https://doi.org/10.1016/0040-6031\(74\)85073-2](https://doi.org/10.1016/0040-6031(74)85073-2).
- [21] M.J. Richardson, N.G. Savill, Temperatures in differential scanning calorimetry, *Thermochim. Acta* 12 (1975) 213–220, [https://doi.org/10.1016/0040-6031\(75\)85033-7](https://doi.org/10.1016/0040-6031(75)85033-7).
- [22] J.H. Flynn, Analysis of DSC results by integration, *Thermochim. Acta* 217 (1993) 129–149, [https://doi.org/10.1016/0040-6031\(93\)85104-H](https://doi.org/10.1016/0040-6031(93)85104-H).
- [23] J.G. Dunn, Recommendations for reporting thermal-analysis data, *J. Therm. Anal.* 40 (1993) 1431–1436, <https://doi.org/10.1007/Bf02546907>.
- [24] T. Ozawa, K. Kanari, Heat capacity measurements by dynamic differential scanning

- calorimetry, *Thermochim. Acta* 288 (1996) 39–51, [https://doi.org/10.1016/S0040-6031\(96\)03029-8](https://doi.org/10.1016/S0040-6031(96)03029-8).
- [25] P.J. Haines, M. Reading, F.W. Wilburn, Differential thermal analysis and differential scanning calorimetry, in: M.E. Brown (Ed.), *Handbook of Thermal Analysis and Calorimetry*, Elsevier, Amsterdam, 1998, pp. 279–362.
- [26] J.A. Martinho Simões, M.E. Minas da Piedade, *Molecular Energetics Condensed Phase Thermochemical Techniques*, Oxford University Press, New York, 2008.
- [27] M.J. Richardson, The application of differential scanning calorimetry to the measurement of specific heat, in: K.D. Maglic, A. Cezairliyan, V.E. Peletsky (Eds.), *Compendium of Thermophysical Properties Measurement Methods*, Plenum, New York, 1992, pp. 519–545.
- [28] G. Höhne, W.F. Hemminger, H.-J. Flammersheim, *Differential Scanning Calorimetry*, 2nd ed., Springer, Heidelberg, 2003.
- [29] B. Wunderlich, *Thermal Analysis of Polymeric Materials*, Springer, Heidelberg, 2005.
- [30] K.S. Gavrichev, M.A. Ryumin, A.V. Khoroshilov, A.V. Tyurin, N.N. Efimov, V.M. Gurevich, G.E. Nikiforova, V.N. Guskov, L.N. Golushina, K.I. Bryukhanova, A.P. Kritskaya, Thermodynamic properties and phase transition of monoclinic terbium orthophosphate, *Thermochim. Acta* 641 (2016) 63–70, <https://doi.org/10.1016/j.tca.2016.08.008>.
- [31] A. Joseph, C.E.S. Bernardes, M.E. Minas da Piedade, Heat capacity and thermodynamics of solid and liquid pyridine-3-carboxylic acid (nicotinic acid) over the temperature range 296 K–531 K, *J. Chem. Thermodyn.* 55 (2012) 23–28, <https://doi.org/10.1016/j.jct.2012.06.010>.
- [32] D.C. Ginnings, G.T. Furukawa, Heat capacity standards for the range 14–1200 K, *J. Am. Chem. Soc.* 75 (1953) 522–527, <https://doi.org/10.1021/ja01099a004>.
- [33] R. Sabbah, X.W. An, J.S. Chickos, M.L.P. Leitao, M.V. Roux, L.A. Torres, Reference materials for calorimetry and differential thermal analysis, *Thermochim. Acta* 331 (1999) 93–204, [https://doi.org/10.1016/S0040-6031\(99\)00009-X](https://doi.org/10.1016/S0040-6031(99)00009-X).
- [34] G. Della Gatta, M.J. Richardson, S.M. Sarge, S. Stolen, Standards, calibration, and guidelines in microcalorimetry - part 2. Calibration standards for differential scanning calorimetry - (IUPAC Technical Report), *Pure Appl. Chem.* 78 (2006) 1455–1476, <https://doi.org/10.1351/pac200678071455>.
- [35] C.S.D. Lopes, F. Agapito, C.E.S. Bernardes, M.E. Minas da Piedade, Thermochemistry of 4-HOC₆H₄COR (R = H, CH₃, C₂H₅, *n*-C₃H₇, *n*-C₄H₉, *n*-C₅H₁₁, and *n*-C₆H₁₃) compounds, *J. Chem. Thermodyn.* 104 (2017) 281–287, <https://doi.org/10.1016/j.jct.2016.09.026>.
- [36] T.B. Coplen, Y. Shrestha, Isotope-abundance variations and atomic weights of selected elements: 2016 (IUPAC Technical Report), *Pure Appl. Chem.* 88 (2016) 1203–1224, <https://doi.org/10.1515/pac-2016-0302>.
- [37] G.T. Furukawa, R.E. Mccoskey, G.J. King, Calorimetric properties of benzoic acid from 0 K to 410 K, *J. Res. Nat. Bur. Stand.* 47 (1951) 256–261, <https://doi.org/10.6028/jres.047.032>.
- [38] R.L. Powell, W.A. Blanpied, *Thermal Conductivity of Metals and Alloys at Low Temperatures: A Review of the Literature*, National Bureau of Standards, Circular 556, Washington, 1954.
- [39] A. Joseph, C.E.S. Bernardes, M.E. Minas da Piedade, Unpublished results.
- [40] M.J. Richardson, E.L. Charsley, Calibration and standardisation in DSC, in: M.E. Brown (Ed.), *Handbook of Thermal Analysis and Calorimetry*, Elsevier, Amsterdam, 1998, pp. 547–575.